19. E. Y. Huang *et al.*, *J. Bacteriol.* **179**, 5648 (1997).
20. Y. A. Hannun, C. Luberto, *Trends Cell Biol.* **10**, 73 (2000).
21. P. W. van der Wielen *et al.*, *Science* **307**, 121 (2005).
22. M. M. Yakimov *et al.*, *Curr. Opin. Biotechnol.* **18**, 257 (2007).
23. A. F. Pronk *et al.*, *J. Bacteriol.* **177**, 75 (1995).
24. O. V. Golyshina, K. N. Timmis, *Environ. Microbiol.* **7**, 1277 (2005).
25. D. A. Pearce, F. Sherman, *J. Bacteriol.* **181**, 4774 (1999).
26. J. D. Woodson *et al.*, *J. Bacteriol.* **185**, 7193 (2003).
27. Y. Jiao *et al.*, *Appl. Environ. Microbiol.* **71**, 4487 (2005).
28. This research was supported by the BIO2006-11738, CSD2007-00005, GEN2006-27750-C-4-E, BFU2008-04398-E/BMC, and KBBE-226977 projects. A.B and Y.A-R thank the Spanish MEC for the FPU and FPI fellowships. F.P. thanks the Spanish MEC for the BIO2006-15318 project. K.N.T, O.V.G., and P.N.G acknowledge the Federal Ministry for Science and Education (BMBF) for a grant in the framework of the BiotechGenoMik program, and K.N.T. thanks the Fonds der Chemischen Industrie for generous support. Authors are deeply indebted to A. Yanenko for sampling Kolguev Island coastal water and to the captain and crew of Research Vessel Urania for their assistance in deep-sea sampling in the Mediterranean Sea and to J. Manuel Franco for statistical analyses.

**Supporting Online Material**
www.sciencemag.org/cgi/content/full/326/5950/252/DC1
Materials and Methods
SOM Text
Figs. S1 to S14
Tables S1 to S6
References
Movie S1

26 March 2009; accepted 19 August 2009
10.1126/science.1174094

# Unbiased Reconstruction of a Mammalian Transcriptional Network Mediating Pathogen Responses

**Ido Amit,[1,2,3,4] Manuel Garber,[1]* Nicolas Chevrier,[2,3]* Ana Paula Leite,[1,5]* Yoni Donner,[1]* Thomas Eisenhaure,[2,3] Mitchell Guttman,[1,4] Jennifer K. Grenier,[1] Weibo Li,[2,3] Or Zuk,[1] Lisa A. Schubert,[6] Brian Birditt,[6] Tal Shay,[1] Alon Goren,[1,7] Xiaolan Zhang,[1] Zachary Smith,[1] Raquel Deering,[2,3] Rebecca C. McDonald,[2,3] Moran Cabili,[1] Bradley E. Bernstein,[1,3,7] John L. Rinn,[1] Alex Meissner,[1] David E. Root,[1] Nir Hacohen,[1,2,3]†‡ Aviv Regev[1,4,8]‡**

Models of mammalian regulatory networks controlling gene expression have been inferred from genomic data but have largely not been validated. We present an unbiased strategy to systematically perturb candidate regulators and monitor cellular transcriptional responses. We applied this approach to derive regulatory networks that control the transcriptional response of mouse primary dendritic cells to pathogens. Our approach revealed the regulatory functions of 125 transcription factors, chromatin modifiers, and RNA binding proteins, which enabled the construction of a network model consisting of 24 core regulators and 76 fine-tuners that help to explain how pathogen-sensing pathways achieve specificity. This study establishes a broadly applicable, comprehensive, and unbiased approach to reveal the wiring and functions of a regulatory network controlling a major transcriptional response in primary mammalian cells.

Regulatory networks controlling gene expression serve as decision-making circuits within cells. For example, when immune dendritic cells (DCs) are exposed to viruses, bacteria, or fungi, they respond with transcriptional programs that are specific to each pathogen (*1*) and are essential for establishing appropriate immunological outcomes (*2*). These responses are initiated through specific receptors, such as Toll-like receptors (TLRs), that distinguish broad pathogen classes and are propagated through well-characterized signaling cascades (*2*). However, little is known about how the transcriptional network is wired to produce specific outputs.

Two major observational strategies have associated regulators with their putative targets on a genome scale (*3*): Cis-regulatory models rely on the presence of predicted transcription factor binding sites in the promoters of target genes (*3*–*5*), whereas trans-regulatory models are based on correlations between regulator and target expression (*3*–*6*). Because promoter binding sites and correlated expression are weak predictors of functional regulator-target linkages, such approaches are limited in their ability to produce reliable models of transcriptional networks (*3*). A complementary strategy is to systematically perturb every regulatory input and measure its effect on the expression of gene targets. This strategy has been successfully used in yeast (*7*–*9*) and sea urchin (*10*), but not in mammals.

**A perturbation-based strategy for network reconstruction.** We developed a perturbation strategy for reconstructing transcriptional networks in mammalian cells and used it to determine a network controlling the responses of DCs to pathogens (Fig. 1). First, we profiled gene expression at nine time points after stimulation with five pathogen-derived components and identified specific and shared genes that respond to each stimulus (fig. S1A). We used these profiles to identify 144 candidate regulators whose expression changed in response to at least one stimulus (*11*) (fig. S1B, top). We also identified a signature of 118 marker genes (fig. S1B, bottom) that captures the complexity of the response. We generated a validated lentiviral short hairpin RNA (shRNA) library for 125 of the 144 candidate regulators (fig. S1C, top), used it to systematically perturb each of the regulators in DCs, stimulated the cells with a pathogen component, and profiled the expression of the 118-gene signature (*12*) (fig. S1C, bottom). Finally, we used the measurements from the perturbed cells to derive a validated model of the regulatory network (fig. S1D).

**Gene expression programs in response to TLR agonists.** We measured genome-wide expression profiles in DCs exposed to PAM3CSK4 (PAM), a synthetic mimic of bacterial lipopeptides; polyinosine-polycytidylic acid [poly(I:C)], a viral-like double-stranded RNA; lipopolysaccharide (LPS), a purified component from Gram-negative *Escherichia coli*; gardiquimod, a small-molecule

[1]Broad Institute of MIT and Harvard, 7 Cambridge Center, Cambridge, MA 02142, USA. [2]Center for Immunology and Inflammatory Diseases, Massachusetts General Hospital, 149 13th Street, Charlestown, MA 02129, USA. [3]Harvard Medical School, Boston, MA 02115, USA. [4]Department of Biology, Massachusetts Institute of Technology, Cambridge, MA 02142, USA. [5]Computational and Systems Biology, Massachusetts Institute of Technology, Cambridge, MA 02139, USA. [6]NanoString Technologies, 530 Fairview Avenue N., Suite 2000, Seattle, WA 98109, USA. [7]Molecular Pathology Unit and Center for Cancer Research, Massachusetts General Hospital, Charlestown, MA 02129, USA. [8]Howard Hughes Medical Institute.
*These authors contributed equally to this work.
†To whom correspondence should be addressed. E-mail: nhacohen@partners.org
‡These authors contributed equally to this work.

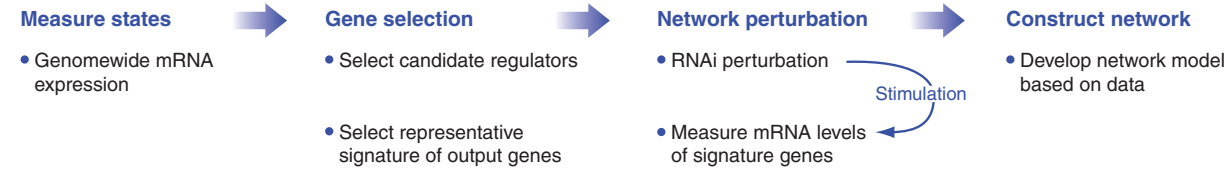


**Fig. 1.** A systematic strategy for network reconstruction. The strategy consists of four steps (left to right): state measurement using arrays; selection of regulators and response signatures; network perturbation with shRNAs against each regulator, followed by measurement of signature genes; and network reconstruction from the perturbational data.

agonist; and CpG, a synthetic single-stranded DNA. These compounds are known agonists of TLR2, TLR3, TLR4, TLR7, and TLR9, respectively. Poly(I:C) also activates the cytosolic viral RNA sensor MDA-5, and LPS can also act through co-receptors such as CD14; we therefore refer to the ligands rather than their receptors for clarity. On the basis of pilot experiments (fig. S2) (*11*), we measured mRNA expression at 0.5, 1, 2, 4, 6, 8, 12, 16, and 24 hours after stimulation with these pathogen components.

The observed transcriptional responses were classified into a "PAM-like" program and a "poly(I:C)-like" program, as well as a shared response [24.5% shared by PAM, poly(I:C), and LPS]. The LPS response (Fig. 2 and fig. S3) was largely the union of the "PAM-like" and "poly(I:C)-like" programs. This is partly explained by the known signaling pathways activated by these agonists. PAM binds TLR2 and signals through the MYD88 pathway; poly(I:C) binds TLR3 and MDA-5 and signals mostly through the TRIF and IPS-1 pathways, respectively; and LPS binds TLR4 and co-receptors and uses the MYD88 and TRIF pathways (*13*). It is also consistent with the known induction of an antiviral response by poly (I:C) and LPS (*14*). The "PAM-like" program is enriched for targets of the transcription factor NF-κB and for inflammatory responsive genes ($P < 6.1 \times 10^{-8}$), whereas the "poly(I:C)-like" program is enriched for interferon regulatory factors (IRFs) and for viral- and interferon-responsive genes (ISGs; $P < 8.3 \times 10^{-24}$). We thus term them the "inflammatory-like" and "antiviral-like" programs. A small number of genes are specific to a single stimulus. For example, ~250 genes are poly(I:C)-specific (1250 are shared with LPS), including several type I interferons (e.g., IFNA2, IFNA4; Fig. 2A). Surprisingly, 82% of the gardiquimod (TLR7) and CpG (TLR9) response was shared with the LPS response, but with a weaker antiviral component (fig. S4). This observation is unexpected given their different signaling mechanisms (*15*), but is highly reproducible and robust (fig. S4) (*11*).

**Identification of candidate regulators and a response signature.** To select potential regulators that mediate the observed transcriptional response, we focused on regulator genes whose expression changes during pathogen sensing [a reasonable assumption for many mammalian responses (*16*, *17*), including pathogen sensing (*1*, *4*)]. First, we reconstructed an observational trans-model of gene regulation (fig. S1B, top, and fig. S5A) (*11*) that associated 80 modules of co-regulated genes with 608 predictive regulators (fig. S5B) (*4*, *11*, *18*, *19*) automatically chosen out of a curated list of 3287 candidate regulators (*11*). Filtering identified 117 regulators above a minimal expression signal in at least one experiment (fig. S5B). These included known regulators from the NF-κB, STAT, and IRF families, as well as unexpected candidates such as the circadian regulator Timeless and the DNA methyltransferase Dnmt3a. Second, we added five constitutively expressed regulators whose cis-regulatory elements are enriched in the responsive genes (*11*). Third, to capture delayed responses or nonlinear relations, we incorporated 22 regulators whose expression changed by at least a factor of 2. This resulted in 144 candidate regulators, with a distribution of expression patterns similar to the general response (figs. S6 to S8 and table S1). The regulators' expression under LPS was conserved between DCs and functionally similar macrophages (Pearson correlation $r = \sim 0.9$ at 1 hour; fig. S9A) as well as between human macrophages and mouse DCs ($r = \sim 0.6$ at 2 hours; fig. S9B), supporting the functional relevance of the regulators' transcription.

To identify highly informative reporter genes for monitoring the effects of perturbing regulators, we devised GeneSelector (fig. S10A and table S2) (*11*). GeneSelector incrementally chooses genes (from our full expression data set) whose expression profile improves our discrimination of stimuli given the previously chosen genes. Using this approach, we identified the optimal time point (6 hours after activation; fig. S10B) and a set of 81 genes that distinguished the stimuli (*11*). We added 37 candidate regulators with

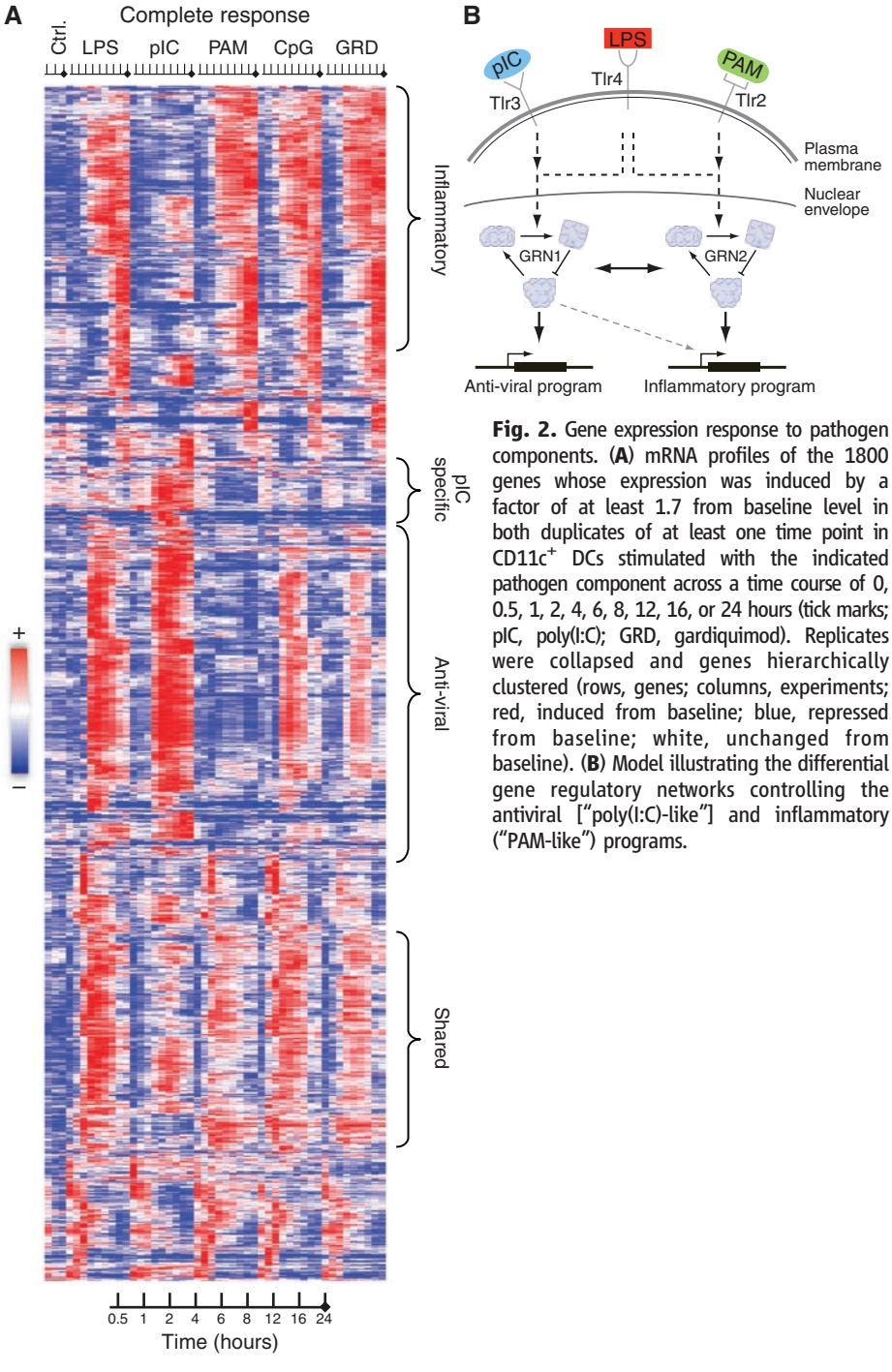


**Fig. 2.** Gene expression response to pathogen components. (**A**) mRNA profiles of the 1800 genes whose expression was induced by a factor of at least 1.7 from baseline level in both duplicates of at least one time point in CD11c$^+$ DCs stimulated with the indicated pathogen component across a time course of 0, 0.5, 1, 2, 4, 6, 8, 12, 16, or 24 hours (tick marks; pIC, poly(I:C); GRD, gardiquimod). Replicates were collapsed and genes hierarchically clustered (rows, genes; columns, experiments; red, induced from baseline; blue, repressed from baseline; white, unchanged from baseline). (**B**) Model illustrating the differential gene regulatory networks controlling the antiviral ["poly(I:C)-like"] and inflammatory ("PAM-like") programs.

detectable expression at the 6-hour time point, creating a signature of 118 genes. Finally, we added 10 control genes whose expression levels were unchanged under all stimuli, but whose (constant) basal levels varied from very low to high.

**Perturbations, profiling, and modeling.** We generated validated lentiviral shRNAs that knocked down the expression of 125 of our 144 candidate regulators in bone marrow DCs by at least 75% (fig. S11 and table S3) (*11*) and 32 shRNAs with no known gene targets as controls (figs. S12 and S13 and table S4) (*11*). To carry out our perturbational study, we selected a single treatment, LPS, that activates the majority of both the "inflammatory-like" and "antiviral-like" programs. After stimulation of shRNA-perturbed DCs with LPS for 6 hours, we used nCounter (*12*) to count transcripts of the 118 reporter and 10 control genes.

The changes in signature gene expression resulting from infection with each shRNA were used to construct a model that associated regulators to their targets. We expected increases in the transcript levels of reporter genes whose repressors are targeted by knockdown, and decreases in reporters whose activators are targeted. Our false discovery rate (FDR) model estimates the statistical significance of a change in transcripts in DCs infected with a given shRNA (*11*). We controlled for gene-specific noise by comparing to changes in the expression of each gene after perturbation with the control shRNAs (Fig. 3A), and for shRNA-specific noise by comparing to changes in the expression of the control genes after a given shRNA perturbation (Fig. 3B). We estimated the sensitivity of our calls from the 37 regulators, which are also included as target reporters (fig. S14) (*11*).

On the basis of these results, we identified a densely overlapping network with 2322 significant regulatory connections, including 1728 activations and 594 repressions (Fig. 3B, red and blue, respectively, at 95% confidence; tables S5 to S7). Of the 125 tested regulators, we confidently identified 100 with at least four targets. Among those were 24 hub regulators that were predicted to regulate more than 25% of the 118 genes measured, as well as 76 specific regulators each affecting the expression of 4 to 25 genes. On average, ~14 (±8; SD) regulators activated a target gene, and 5 (±5.8) regulators repressed it. Indirect effects may account for the large number of regulators we observed for each target.

Our perturbational model captured known regulatory features of the response, but also identified novel regulators. The reporter genes partitioned into two main clusters according to their response to perturbations (Fig. 3B and fig. S15A), consistent with the expression data: the "antiviral poly(I:C)–like" program reporters (e.g., Cxcl10, Isg15, and Ifit1) and the "inflammatory (PAM)–like" program reporters [e.g., IL1b, Cxcl2, IL6, and IL12b). We also found many known regulatory relations—for example, the NF-κB family of transcription factors (Rel, Rela, Relb, Nfkb1, Nfkb2, and Nfkbiz) regulating their known inflammatory gene targets. Our network provided evidence for the involvement of at least 68 additional regulators in the response to pathogens, of which 11 were hubs not previously associated with this system. Interestingly, 12 of the identified regulators (e.g., Hhex, Fus, Bat5, and Pa2g4) are in linkage disequilibrium with single-nucleotide polymorphisms (SNPs) associated with autoimmune and related diseases in genome-wide association studies (table S8).

**The core inflammatory and antiviral programs.** We next addressed how each regulator contributes to the generation of specific cell states. We first automatically defined the two major states induced by the five pathogen components with the use of non-negative matrix factorization (NMF) (*20*) and the original array data (*11*). This procedure identified two major expression components (termed "metagenes"): one predominantly determined by genes from the "inflammatory-like" program and the other by genes from the "antiviral-like" programs (Fig. 2A). Next, we quantified the effects of each regulator's knockdown on these two states (Fig. 3B, fig. S15A, and table S9) by classifying the nCounter expression measurements after a regulator's perturbation (*20*, *21*).

Finally, we used a regulator ranking score (*11*) to assign 33 (8 known) genes as regulators of the inflammatory state and 33 (15 known) genes as regulators of the antiviral state. This accurately classified the known activators of the inflammatory response (e.g., the NF-κB factors Rela, Nfkbiz, and Nfkb1; Fig. 3C, yellow in the inflammatory metagene) and of the antiviral response (e.g., Stat1, Stat2, Stat4, Irf8, and Irf9; Fig. 3C, yellow in the viral metagene). Although all perturbation experiments were conducted only under LPS stimulation (a bacterial component), we correctly classified factors known to mediate the response to other stimuli. Because 34 additional regulators were associated with both responses, it is possible that a single regulator can control genes in either state, depending on the differential timing of regulator activation, its level, or combinatorial regulation. Notably, for 12 of the transcription factors examined, we found an enriched cis-regulatory element in the appropriate metagene (*11*).

On the basis of the NMF scores (table S9), we identified an inflammatory subnetwork (fig. S15B), an antiviral subnetwork (Fig. 4A and fig. S15C), and several fine-tuning subnetworks that affect smaller numbers of genes from both responses (figs. S15D and S16) (*11*). The inflammatory subnetwork (fig. S15B) consisted of three regulatory modes: dominant activators (Cebpb, Bcl3, and Cited2) that induce more inflammatory targets than antiviral ones; cross-inhibitors (Nfkbiz, Nfkb1, Atf4, and Pnrc2) that induce inflammatory genes while repressing antiviral ones; and specific activators (Runx1 and Plagl2) that almost entirely target inflammatory genes. We observed that dominant activators mostly regulate effectors, whereas regulators are primarily controlled by cross-inhibitors.

Focusing on the network architecture, we found multiple feedforward circuits in this response, where an upstream regulator controls a target gene both directly and indirectly through a secondary regulator (*22*) (e.g., Fig. 4B and tables S10 and S11). The majority (76%, 4892 of 6444) of these feedforward circuits were found to be coherent (*22*), having the same direct and indirect effect on the regulated gene. The vast majority (80%) are type I loops (*23*) (Fig. 4B) with all-positive regulation (e.g., Nfkbiz activates E2f5 and both activate IL-6). Such feedforward circuits respond to persistent rather than transient stimulation, protecting the system from responding to spurious signals, as was shown for one circuit in LPS-stimulated macrophages (*24*). Our finding suggests that coherent feedforward loops, especially class I (*22*), are a general design principle in this system and may have a physiological impact on this response.

In the antiviral subnetwork, we identified a two-tiered regulatory circuit combining feedforward and feedback loops (Fig. 4A and table S11). This circuit has at the top the antiviral regulators Stat1 and Stat2, which regulate a full complement of antiviral reporters. The second-tier regulators Timeless, Rbl1, and Hhex are controlled by Stat1 and Stat2 and most likely form coherent feedforward loops that target specific subsets of genes. Timeless, Rbl1, and Hhex also feed back and promote the expression of the Stat regulators. This circuit is repressed through the cell cycle regulator and RNA binding protein Fus (*25*), acting as a single dominant inhibitor of 43 viral genes.

Finally, we derived a core network incorporating the regulators with the most substantial impact on each response, on the basis of the number, magnitude, and logic of targets that each regulator affects (*11*). The core network (Fig. 4C) has 24 regulators, 13 of which have previously been identified as key factors regulating the inflammatory or antiviral responses; the other 11 have not been previously implicated in either response. Of these 24 regulators, 19 are transcription factors, three are chromatin modifiers, and two are RNA binding proteins. The regulators apparently distinguish the two programs through cross-inhibition (Fig. 4C, gray lines) or dominant activation (Fig. 4C). The core network also explains how differential expression of secreted factors is specified, leading to the activation and migration of appropriate cell types for different pathogens (*11*, *26*) (fig. S17).

Embedded within the many known regulators of the antiviral response (Fig. 4C and fig. S15C), we found a large set of regulators not previously associated with this response. These included several known regulators of the cell cycle and the circadian rhythm, including Rbl1, Jun, Rb, E2f5, E2f8, Nmi, Fus, and Timeless, several of which were placed in our core network. This

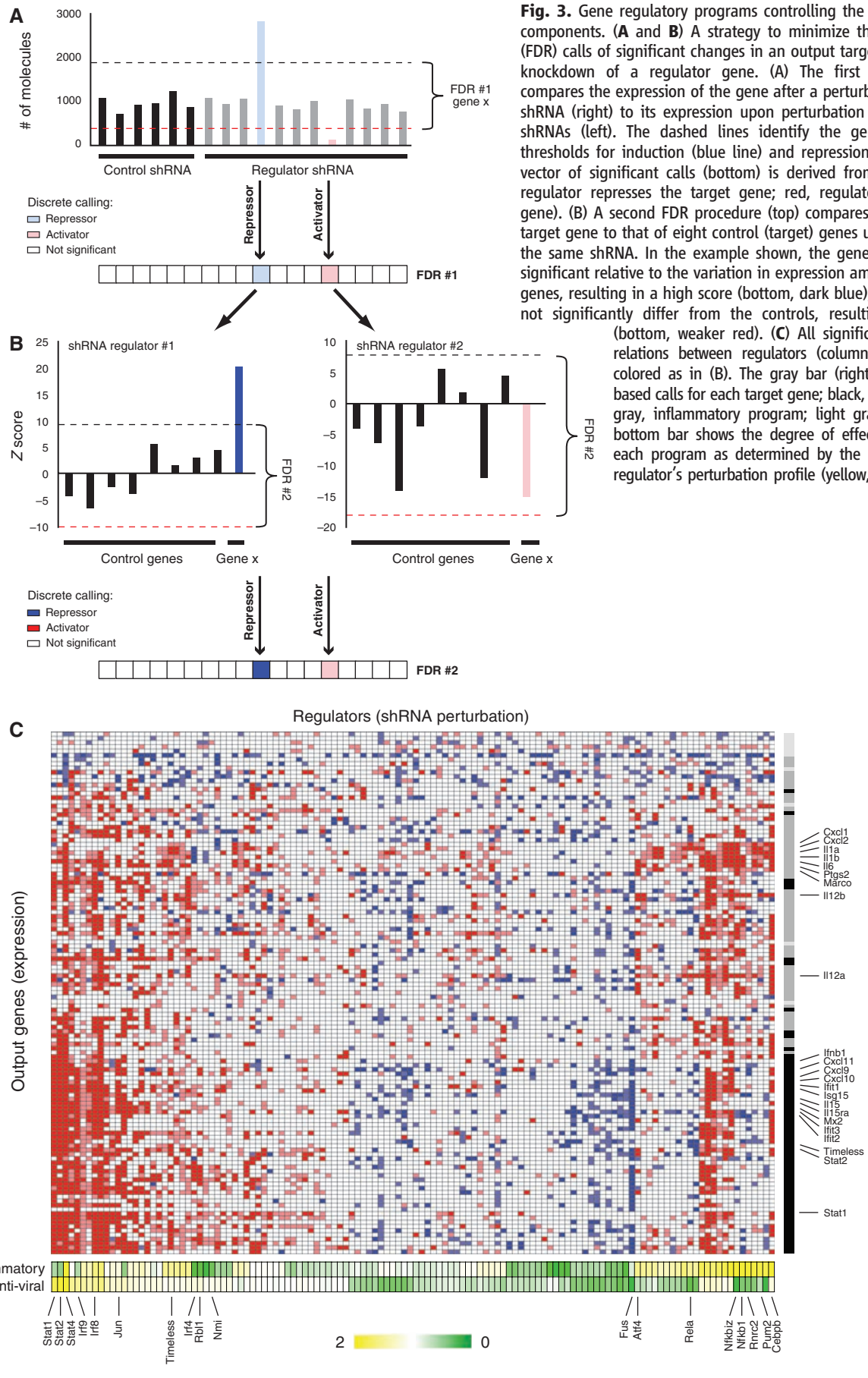


**Fig. 3.** Gene regulatory programs controlling the response to pathogen components. (**A** and **B**) A strategy to minimize the false discovery rate (FDR) calls of significant changes in an output target gene resulting from knockdown of a regulator gene. (A) The first FDR procedure (top) compares the expression of the gene after a perturbation with a regulator shRNA (right) to its expression upon perturbation with 32 nontargeting shRNAs (left). The dashed lines identify the gene-specific FDR-based thresholds for induction (blue line) and repression (red line). A discrete vector of significant calls (bottom) is derived from the raw data (blue, regulator represses the target gene; red, regulator induces the target gene). (B) A second FDR procedure (top) compares the expression of the target gene to that of eight control (target) genes upon perturbation with the same shRNA. In the example shown, the gene's induction (left) was significant relative to the variation in expression among the control target genes, resulting in a high score (bottom, dark blue), but its repression did not significantly differ from the controls, resulting in a lower score (bottom, weaker red). (**C**) All significant (95% confidence) relations between regulators (columns) and targets (rows), colored as in (B). The gray bar (right) represents the NMF-based calls for each target gene; black, antiviral program; dark gray, inflammatory program; light gray, control genes. The bottom bar shows the degree of effect by the regulator on each program as determined by the NMF projection of the regulator's perturbation profile (yellow, high; green, low).

suggests that a cell cycle regulatory circuit was co-opted to function in the antiviral response in DCs (with no observable effect on cell cycle progression; fig. S18). Because we identified these antiviral regulatory relations in perturbation experiments using DCs stimulated with the bacterial component LPS, we silenced four regulators (Timeless, Rbl1, Jun, and Nmi) after exposure to the viral component poly(I:C). Each of the four regulators had a strong impact on the antiviral program, more than was observed under LPS stimulation (Fig. 4D), and on affected genes (e.g., type I IFNs) whose expression is poly(I:C)-specific. Nmi affected a smaller set of genes, consistent with the model's prediction. These results demonstrate our ability to correctly predict function in unobserved conditions.

Although most antiviral genes are induced after stimulation with the bacterial component LPS, a few critical ones are expressed specifically in poly(I:C) stimulation or follow distinct patterns in each stimulus. For example, in response to viral infection, cells induce the production of interferon β1 (Ifnb1), a crucial mediator of the antiviral response. Because high levels of Ifnb1 may be deleterious to the host if infected by specific bacteria (*27*), we predicted that specific mechanisms insulate Ifnb1's regulation from the response to LPS. Indeed, although Ifnb1 expression was induced in the first 2 hours of stimulation with LPS, this expression declined at subsequent time points, in contrast to its sustained induction after poly(I:C) treatment (Fig. 5A). Our model suggested that three regulators known to affect chromatin remodeling (*25*, *28*, *29*) are Ifnb1 repressors in LPS (Fig. 5B): the Polycomb complex subunit Cbx4 (*28*), Fus (*25*), and the DNA methyltransferase Dnmt3a (*29*). Cbx4 appeared to confer antiviral specificity to Ifnb1 induction because it was induced within the first 2 hours of PAM and LPS treatment but not by poly(I:C) (Fig. 5C), and Cbx4 knockdown caused induction of Ifnb1 mRNA and protein during LPS treatment (Fig. 5D and fig. S19A) but had no effect on the induction of the chemokine Cxcl10, a poly(I:C)- and LPS-induced gene (fig. S19B). Cbx4 knockdown did not affect Ifnb1 during PAM activation (Fig. 5E), when the antiviral response is not induced. Combined with evidence for chromatin changes around the Ifnb1 locus and its closest neighbor gene, Ptplad2 (fig. S20A), which has a similar dependence on Cbx4, these data are consistent with an effect by Cbx4 on local chromatin organization (fig. S20, B and C). Cbx4 knockdown affected few genes (~120 up-regulated and ~120 down-regulated genome-wide; table S12). Because most up-regulated

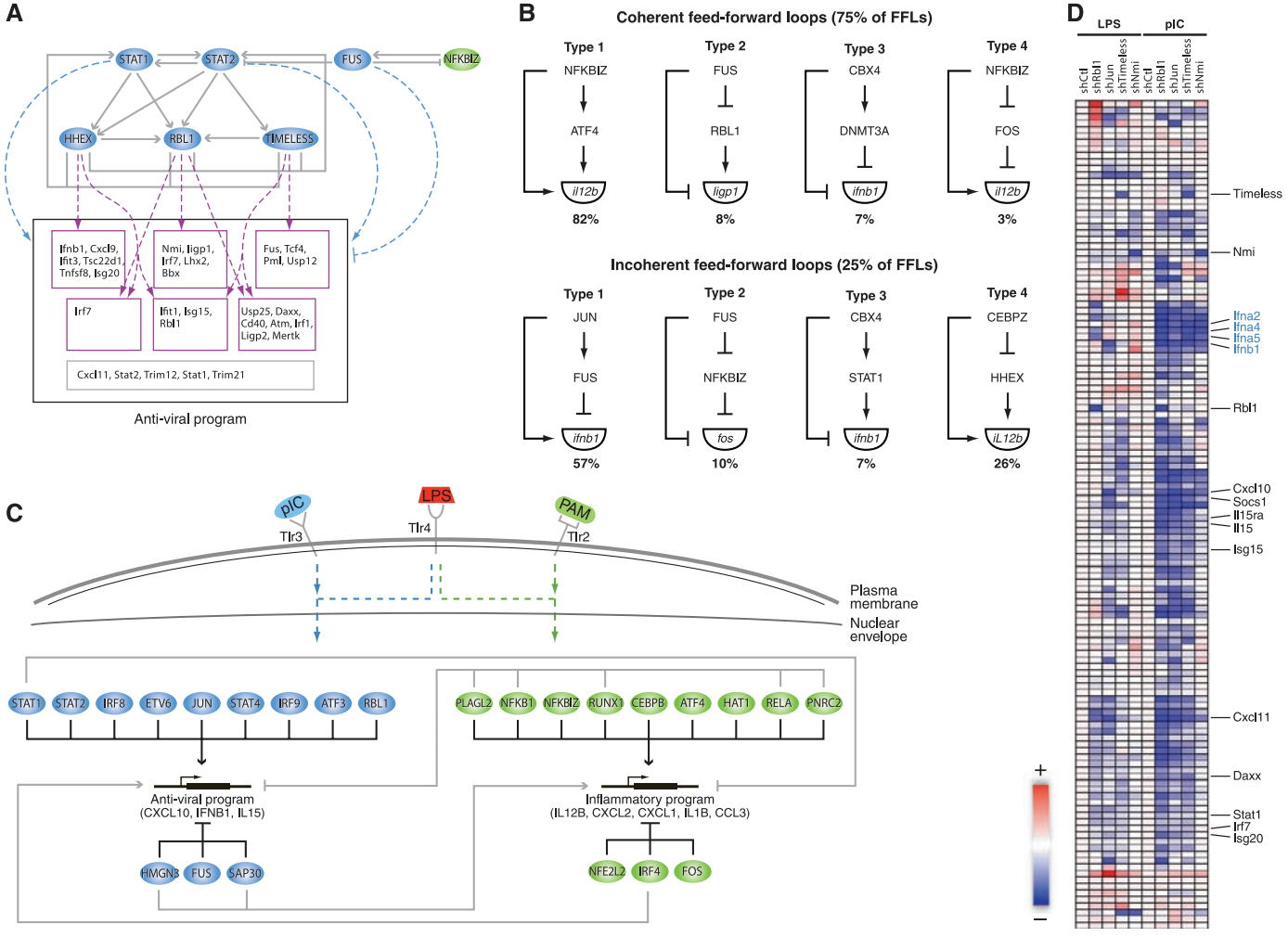


**Fig. 4.** The core regulatory circuits controlling the inflammatory and antiviral responses. (**A**) The antiviral subnetwork shows regulatory relations between the core antiviral regulators (blue nodes, top), their targets (boxes, bottom), each other, and inflammatory regulators (green node, top right). The two top regulators, Stat1 and Stat2, activate all antiviral targets (dashed blue arrows). The second-tier regulators activate subsets of targets (dashed purple arrows). (**B**) Examples of feedforward loop classes identified in the network, with fraction of each class. (**C**) A core regulatory network of the inflammatory and antiviral programs, consisting of the most distinct regulators, and their relation to ligands and receptors (top). Pointed arrows, induction; blunt arrows, repression; green ovals, inflammatory regulators; blue ovals, antiviral regulators. Example target genes are noted. (**D**) nCounter expression profiles for the target genes (rows) upon perturbation with shRNAs against a subset of viral regulators (columns) and followed by stimulation with LPS (left) or poly(I:C) (right). All values are normalized by expression in cells infected with a control shRNA and under the same stimulus (shCtl).

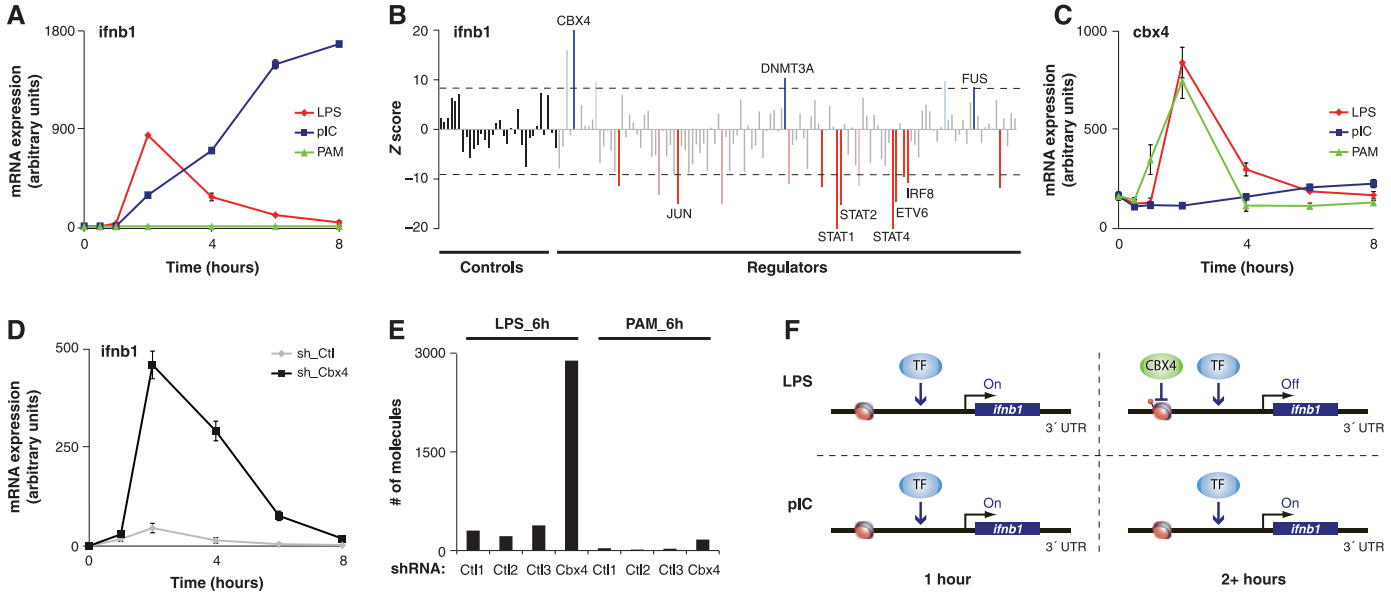


**Fig. 5.** The polycomb component Cbx4 selectively restricts Ifnb1 production under bacterial perturbations. (**A** and **C**) LPS (red), poly(I:C) (blue), and PAM (green)–induced expression of Ifnb1 (A) and Cbx4 (C) derived from data in Fig. 2A. (**B**) Ifnb1 expression (by nCounter) in response to LPS in DCs perturbed by control shRNAs or shRNAs targeting each of 125 regulators (format as in Fig. 3B). (**D**) Ifnb1 mRNA levels (by quantitative reverse transcription polymerase chain reaction) after LPS treatment in unsorted mouse bone marrow DCs perturbed with an shRNA against Cbx4 (black) or a control shRNA (gray); signals are relative to $t = 0$. (**E**) Ifnb1 mRNA levels (by nCounter) at 6 hours after exposure to LPS or PAM in bone marrow DCs perturbed with an shRNA against Cbx4 or one of three control shRNAs. (**F**) Model for bacterial-specific repression of Ifnb1 by Cbx4. Both poly(I:C) and LPS induce Ifnb1 expression early (left), but only LPS induces Cbx4, which then represses the *Ifnb1* locus at a later time (right, top).

genes show a precise temporal pattern in unperturbed cells akin to that of Cbx4—they are induced quickly and return to basal level by 2 to 4 hours (fig. S21, A to F)—we conclude that a chromatin modifier can act like a transcription factor controlling the precise expression of specific genes in the regulatory program.

Taken together, our results suggest a model of a transcriptional negative feedback loop, controlling Ifnb1 expression in LPS stimulation, wherein the induced proinflammatory regulator and chromatin modifier Cbx4 represses transcription by modifying the chromatin in the Ifnb1 locus, generating the specificity needed to drive the inflammatory versus the antiviral response (Fig. 5F). The type III coherent feedforward loop formed by Cbx4 and Dnmt3a (Fig. 4B) is consistent with a delayed repression of Ifnb1. Because neither regulator carries a sequence-specific DNA binding domain, the factors responsible for their guidance to the *Ifnb1* locus remain unknown.

**Discussion.** A central goal of our study was to address the mechanistic basis for pathogen-specific responses. Consistent with previous studies (*14*), we distinguished two key programs, a PAM (TLR2)–like inflammatory response and a poly(I:C) (TLR3/MDA-5)–like antiviral response, which are together induced by LPS, a Gram-negative bacterial component and a TLR4 ligand. These programs reflect both qualitative and quantitative differences between the required functional responses, and are consistent with the cross-protection between certain bacteria and virus infections (*14*). The broad effect of LPS allowed us to focus on a single stimulus and time point, but screens with other stimuli may identify additional unique regulators.

We found that these two responses are controlled by two corresponding regulatory arms, uncovering a mechanistic basis for the observed transcriptional responses. These two arms are integrated into a core network of 24 regulators that balance specific and shared responses through dominant activation and cross-inhibition. In the inflammatory response, we found several feed-forward loops, which may ensure response to only persistent and not sporadic signals. In the antiviral response, we discovered a two-tiered circuit involving feedback and feedforward loops, implicating a module of cell cycle regulators (Jun, Rbl1, Timeless, and Nmi), which we directly validated. More than 75 additional genes work to further fine-tune the regulation of gene targets. This perturbational model identifies many regulatory relations that would have been missed by nonsystematic approaches.

Our work establishes an unbiased, straightforward, and general framework for network reconstruction in mammalian cells (*11*), including several strategies to leverage shRNA for the study of gene regulation. This approach can be executed at substantial scale and reasonable cost, and is compatible with the challenge of deciphering the multiple regulatory systems that operate in mammals. It can be expanded to derive increasingly detailed models and to distinguish direct from indirect targets.

Our study will facilitate the development of new computational approaches to infer regulatory models. Although many computational approaches have attempted to derive observational models, their quality has been difficult to evaluate (*3*). The data generated here include expression profiles for training a model, as well as a perturbational unbiased screen for testing its quality (ftp://ftp.broadinstitute.org/pub/papers/dc_network). When we compared the perturbational model to our observational model, we found that many candidate regulators were correctly identified in both (figs. S5 and S22). However, there were also numerous false positive relations in the observational model, attributable to the fact that both the correct regulator and many others have indistinguishable expression (figs. S22 and S23).

The high-resolution map we constructed has important biomedical implications. By identifying regulators that mediate the differential control of specific gene pairs (e.g., IL-23 versus IL-12, fig. S17) and entire regulatory arms (e.g., viral versus inflammatory), it opens the way for therapeutic targeting of specific pathways to control disease or enhance vaccine efficacy. Furthermore, 12 of our regulators reside in genetic loci that were in linkage disequilibrium with SNPs associated with autoimmune and related diseases. The identified genes and their impact on DCs provide hypotheses to help explain how alleles of genes in a cascade may alter susceptibility to specific infections or immune disorders in humans.

### References and Notes

1. Q. Huang *et al.*, *Science* **294**, 870 (2001).
2. T. Kawai, S. Akira, *Int. Immunol.* **21**, 317 (2009).

3. H. D. Kim, T. Shay, E. K. O'Shea, A. Regev, *Science* **325**, 429 (2009).
4. S. A. Ramsey *et al.*, *PLOS Comput. Biol.* **4**, e1000021 (2008).
5. H. Suzuki *et al.*, *Nat. Genet.* **41**, 553 (2009).
6. E. Segal *et al.*, *Nat. Genet.* **34**, 166 (2003).
7. A. P. Capaldi *et al.*, *Nat. Genet.* **40**, 1300 (2008).
8. Z. Hu, P. J. Killion, V. R. Iyer, *Nat. Genet.* **39**, 683 (2007).
9. C. T. Workman *et al.*, *Science* **312**, 1054 (2006).
10. D. H. Erwin, E. H. Davidson, *Nat. Rev. Genet.* **10**, 141 (2009).
11. See supporting material on *Science* Online.
12. G. K. Geiss *et al.*, *Nat. Biotechnol.* **26**, 317 (2008).
13. J. C. Kagan *et al.*, *Nat. Immunol.* **9**, 361 (2008).
14. S. Doyle *et al.*, *Immunity* **17**, 251 (2002).
15. T. Kawai *et al.*, *Nat. Immunol.* **5**, 1061 (2004).
16. I. Amit *et al.*, *Nat. Genet.* **39**, 503 (2007).
17. D. Pe'er, A. Regev, A. Tanay, *Bioinformatics* **18** (suppl. 1), S258 (2002).
18. S. I. Lee *et al.*, *PLoS Genet.* **5**, e1000358 (2009).
19. H. Zou, T. Hastie, *J. R. Stat. Soc. B* **67**, 301 (2005).
20. J. P. Brunet, P. Tamayo, T. R. Golub, J. P. Mesirov, *Proc. Natl. Acad. Sci. U.S.A.* **101**, 4164 (2004).
21. J. P. Daily *et al.*, *Nature* **450**, 1091 (2007).
22. S. Mangan, U. Alon, *Proc. Natl. Acad. Sci. U.S.A.* **100**, 11980 (2003).
23. U. Alon, *Nat. Rev. Genet.* **8**, 450 (2007).
24. V. Litvak *et al.*, *Nat. Immunol.* **10**, 437 (2009).
25. X. Wang *et al.*, *Nature* **454**, 126 (2008).
26. A. D. Luster, *Curr. Opin. Immunol.* **14**, 129 (2002).
27. T. Decker, M. Muller, S. Stockinger, *Nat. Rev. Immunol.* **5**, 675 (2005).
28. E. Bernstein *et al.*, *Mol. Cell. Biol.* **26**, 2560 (2006).
29. B. Li *et al.*, *Biochem. J.* **405**, 369 (2007).
30. We thank E. Lander, I. Wapinski, D. Pe'er, N. Friedman, J. Kagan, A. Luster, V. Kuchroo, and A. Citri for discussions and comments; L. Gaffney for assistance with artwork; S. Gupta and the Broad Genetic Analysis Platform for microarray processing; and T. Mikkelsen and the Broad Sequencing Platform for help with the ChIP-seq experiments. Supported by the Human Frontier Science Program Organization and a Claire and Emanuel G. Rosenblatt Award from the American Physicians Fellowship for Medicine in Israel (I.A.); NIH grant R21 AI71060 and the NIH New Innovator Award (N.H.); and a Career Award at the Scientific Interface from the Burroughs Wellcome Fund, an NIH Pioneer Award, and the Sloan Foundation (A.R.). A.R. is an Early Career Scientist of the Howard Hughes Medical Institute and an investigator of the Merkin Foundation for Stem Cell Research at the Broad Institute. Complete microarray data sets are available at the Gene Expression Omnibus (accession no. GSE17721).

**Supporting Online Material**

www.sciencemag.org/cgi/content/full/1179050/DC1
Materials and Methods
SOM Text
Figs. S1 to S23
Tables S1 to S16
References

14 July 2009; accepted 26 August 2009
Published online 3 September 2009;
10.1126/science.1179050
Include this information when citing this paper.



# Mapping Excited-State Dynamics by Coherent Control of a Dendrimer's Photoemission Efficiency

**Daniel G. Kuroda,[1]* C. P. Singh,[1]† Zhonghua Peng,[2] Valeria D. Kleiman[1]‡**

Adaptive laser pulse shaping has enabled impressive control over photophysical processes in complex molecules. However, the optimal pulse shape that emerges rarely offers straightforward insight into the excited-state properties being manipulated. We have shown that the emission quantum yield of a donor-acceptor macromolecule (a phenylene ethynylene dendrimer tethered to perylene) can be enhanced by 15% through iterative phase modulation of the excitation pulse. Furthermore, by analyzing the pulse optimization process and optimal pulse features, we successfully isolated the dominant elements underlying the control mechanism. We demonstrated that a step function in the spectral phase directs the postexcitation dynamics of the donor moiety, thus characterizing the coherent nature of the donor excited state. An accompanying pump-probe experiment implicates a 2+1 photon control pathway, in which the optimal pulse promotes a delayed excitation to a second excited state through favorable quantum interference.

Since ancient times, humans have been trying to control the transformation of matter. For more than a century, absorption of light has been used to initiate photochemical reactions. It is only in the past 20 years, however, that researchers have devised techniques to steer the ensuing dynamics through modulation of the optical excitation field. Such quantum, or coherent, control schemes (*1*–*3*) use laser-derived electric fields to direct the motion of wave packets along excited-state potential energy surfaces (*4*–*6*). In principle, the phases and amplitudes in the applied field necessary to achieve a given outcome can be obtained from the field's coupling to the molecular Hamiltonian. In practice, rational design of the requisite pulse shapes remains an insurmountable problem for large molecules in condensed phase: The complete Hamiltonian is either unknown or too complex to be used in electric field calculations. Instead, researchers have relied on empirical methods whereby pulse shapes are determined through iterative optimization using the desired product (e.g., fluorescence quantum yield) as a feedback parameter (*7*). Thus, photoinduced processes can be actively manipulated without previous knowledge of the Hamiltonian and the light-matter couplings (*8*–*11*).

This closed-loop feedback technique has proven powerfully versatile. For example, modulation of isomerization yield in the natural photoreceptor bacteriorhodopsin (*11*), and control of quantum efficiency in both natural and artificial photosynthetic antennae by tuning spectral amplitude and phase in resonant linear excitation (*9*, *12*), were shown. Nonetheless, very few closed-loop experiments have yielded optimal pulse shapes that can be directly explained in terms of known molecular properties of the system under investigation (*9*, *11*, *13*–*15*). Major hindrances to attain such insight are the often intricate relationship between the variables to be optimized and the molecular response; the large number of parameters used for the generation of arbitrarily modulated pulses; and the often arbitrary, random pathways to optimization generated by the iteration algorithms. A major goal in the field is thus to develop a procedure for gleaning molecular insight from coherent control, especially in systems where the photophysical or photochemical pathways are presently unknown. For example, using optimal control, Branderhorst *et al.* (*15*) were able to identify wave packets with minimum position variance as candidates to minimize coupling to the bath and thus increase coherence robustness.

Our approach toward this end is to search for a confined set of parameters that directly govern the optimization. The idea is to express all the independent electric field parameters obtained from the collection of closed-loop optimization data as a combined set, filtering out those variables with redundant or negligible effects on the molecular response (*16*–*20*). Ideally, it ought to be more straightforward to associate these fewer parameters with a physical property.

We apply this approach to coherent control studies of the emissive properties of the phenylene ethynylene dendrimer $2G_2$-m-Per (Fig. 1) (*21*), designed to mimic natural light harvesting systems (*22*). Phenylene ethynylene dendrimers are rigid macromolecules with a high quantum yield for energy transfer from donor to ac-

[1]Department of Chemistry, Center for Chemical Physics, University of Florida, Gainesville, FL 32611–7200, USA. [2]Department of Chemistry, University of Missouri–Kansas City, Kansas City, MO 64110–2499, USA.

*Present address: Department of Chemistry, University of Pennsylvania, Philadelphia, PA 19104–6323, USA.
†On leave from Raja Ramanna. Centre for Advanced Technology, Indore, India.
‡To whom correspondence should be addressed. E-mail: kleiman@chem.ufl.edu

# Unbiased Reconstruction of a Mammalian Transcriptional Network Mediating Pathogen Responses

Ido Amit, Manuel Garber, Nicolas Chevrier, Ana Paula Leite, Yoni Donner, Thomas Eisenhaure, Mitchell Guttman, Jennifer K. Grenier, Weibo Li, Or Zuk, Lisa A. Schubert, Brian Birditt, Tal Shay, Alon Goren, Xiaolan Zhang, Zachary Smith, Raquel Deering, Rebecca C. McDonald, Moran Cabili, Bradley E. Bernstein, John L. Rinn, Alex Meissner, David E. Root, Nir Hacohen and Aviv Regev

*Science* **326** (5950), 257-263.
DOI: 10.1126/science.1179050originally published online September 3, 2009

**Peeking at Pathogen Response Networks**

Networks controlling gene expression serve as key decision-making circuits in cells, but the regulatory networks that control dynamic and specific gene expression responses to stimuli are often not well understood. This is particularly true for immune dendritic cells (DCs), which respond to pathogens by mounting elaborate transcriptional responses, and are centrally involved in infectious diseases, autoimmunity, and vaccines. **Amit *et al.*** (p. 257, published online 3 September) explored the transcriptional response of dendritic cells to specific classes of pathogens. The transcriptional subnetworks responsible for mammalian dendritic cell responses to different pathogens were identified, and the function of 100 regulators clarified.